Laboratory-Scale Penetration Experiments into Geological Targets to Impact Velocities of 2.1 km/s

M. J. Forrestal

Sandia National Laboratories,
Albuquerque, N. Mex. 87185
Mem. ASME

L. M. Lee

B. D. Jenrette

Ktech Corporation,
Albuquerque, N. Mex. 87110

We obtained forces on 3.0 and 6.0 CRH, ogival-nosed projectiles penetrating a simulated geological target. A gas gun and a powder gun accelerated foundry core targets (a simulated soft sandstone) to steady velocities between 0.6–2.1 km/s, and the targets subsequently impacted 20.6 mm diameter penetrators. Rigid-body motions of the penetrators were obtained with laser interferometry and piezoelectric accelerometers. At a penetration velocity of about 1.5 km/s, the 6.0 CRH nose shape exhibited severe, permanent deformation; whereas, the 3.0 CRH nose shape remained undeformed for penetration velocities up to 2.1 km/s.

Introduction

Backman and Goldsmith (1978) and Zukas (1982) discuss many recently developed analytical and experimental methods used to study penetration mechanics. For metal perforation and penetration, laboratory-scale experiments play a dominant role in the research required to understand penetration phenomena. However, experimental work on penetration into geological targets seems to be dominated by full-scale, field tests. Over the last two decades, Young (1969, 1971) and Patterson (see Forrestal, Longcope, and Norwood, 1981) conducted hundreds of instrumented, full-scale, field tests into soil, rock, and sea-ice targets. These penetrators usually contained on-board recording systems and measured deceleration during the penetration event. To complement these full-scale test programs, we have recently devised some laboratory-scale experiments. Forrestal et al. (1984) used gas guns to perform reverse-ballistic experiments with simulated, geological targets. Piezoelectric accelerometers measured the rigid-body acceleration of several nose shapes for impact velocities between 0.2–1.2 km/s. Since current field data are limited to impact velocities less than 0.6 km/s, laboratory-scale experiments can provide time-resolved data for much higher impact velocities.

For the present study, we measured rigid-body penetrator motions with laser interferometry and accelerometers for impact velocities from 0.6 to 2.1 km/s. As in our previous paper (Forrestal et al. 1984), the targets were foundry core samples made at the Sandia foundry. These targets had nominal density 1.8 Mg/m^3 and simulated many of the properties of the
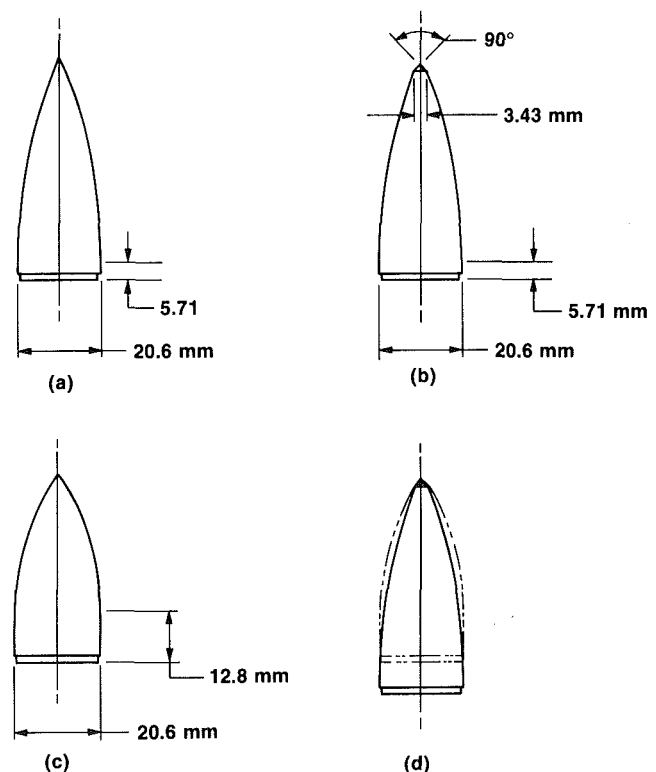
Fig. 1 Penetrator nose shapes: (a) 6.0 CRH; (b) tip-modified 6.0 CRH; (c) 3.0 CRH; (d) overlay of (b) and (c)

natural targets at the Sandia Tonopah Test Range, Nevada. For impact velocities less than 1.2 km/s, we used the Air Force Weapons Laboratory 102 mm bore (4.0 in.) gas gun; and for impact velocities between 1.2–2.1 km/s, we used the Sandia National Laboratories 89 mm bore (3.5 in.) powder gun. For impact velocities above 1.2 km/s, the penetrator accelerations approached the accelerometer capability (10^5 g); and for these
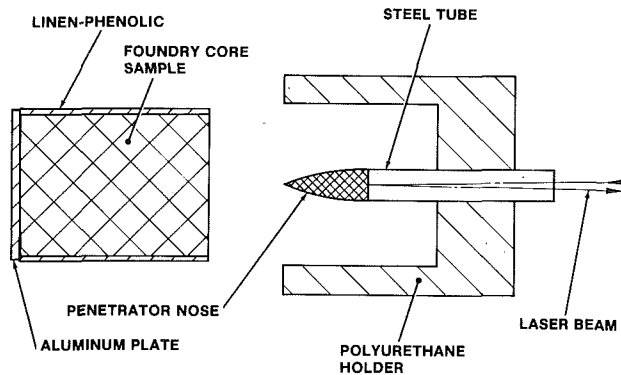
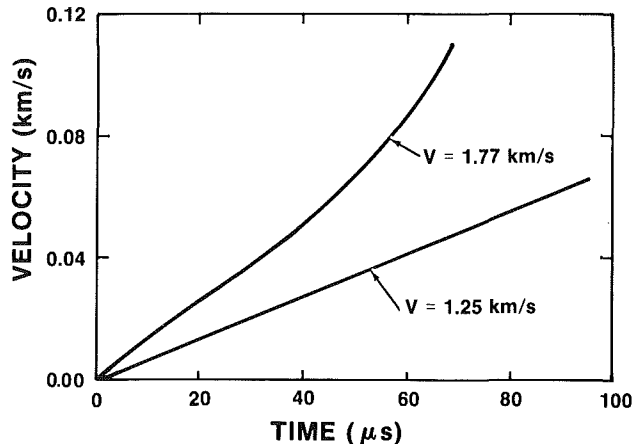Fig. 2 Schematic for the powder-gun, reverse-ballistic experiments

Fig. 3 Rigid-body, velocity-time responses for the 6.0 CRH nose shape. Impact velocities V = 1.25 and 1.77 km/s.

Fig. 4 Post-test nose shapes: (a) top, 6.0 CRH; (b) middle, tip-modified 6.0 CRH; (c) bottom, 3.0 CRH

higher impact velocity experiments, rigid-body motions were measured with laser interferometry (VISAR).

In our previous paper (Forrestal et al., 1984), we performed experiments to impact velocities of 1.2 km/s with two conical nose shapes and a 6.0 CRH ogival nose shape made from a tungsten alloy. For this study, we performed experiments on the same nose material to impact velocities of 2.1 km/s on 3.0 and 6.0 CRH ogival nose shapes. At a penetration velocity of about 1.5 km/s, the 6.0 CRH nose shape exhibited severe, permanent deformation. Brooks (1974) observed this same effect in his study on penetration into metal targets and termed this phenomenon the hydrodynamic transition velocity. By contrast, the 3.0 CRH nose shape remained undeformed for penetration velocities up to 2.1 km/s. In addition, we conducted a few experiments with the nose shape shown in Fig. 1b. This nose has a 6.0 CRH shape except its tip has a blunted, conical shape. The overlay in Fig. 1d shows that this tip-modified 6.0 CRH nose shape has nearly the same geometry as the 3.0 CRH nose shape. We hoped this design modification would avoid the hydrodynamic transition that occurred with the 6.0 CRH nose shape. However, several experiments indicated negligible differences in the motion responses and the hydrodynamic transition velocities for the 6.0 CRH nose shape and the tip-modified 6.0 CRH nose shape.

Experiments

Reverse-Ballistic Experiments. Figure 2 illustrates the reverse-ballistic experimental arrangement. Foundry core samples, contained within hollow projectiles, were accelerated to steady velocities, and the targets subsequently impacted 20.6 mm diameter (0.81 in.) penetrators. The Sandia Foundry made the targets with nearly the same process as that used for making molds for metal castings. This material is a mixture of silica sand (90 percent by weight) and binder ingredients. After
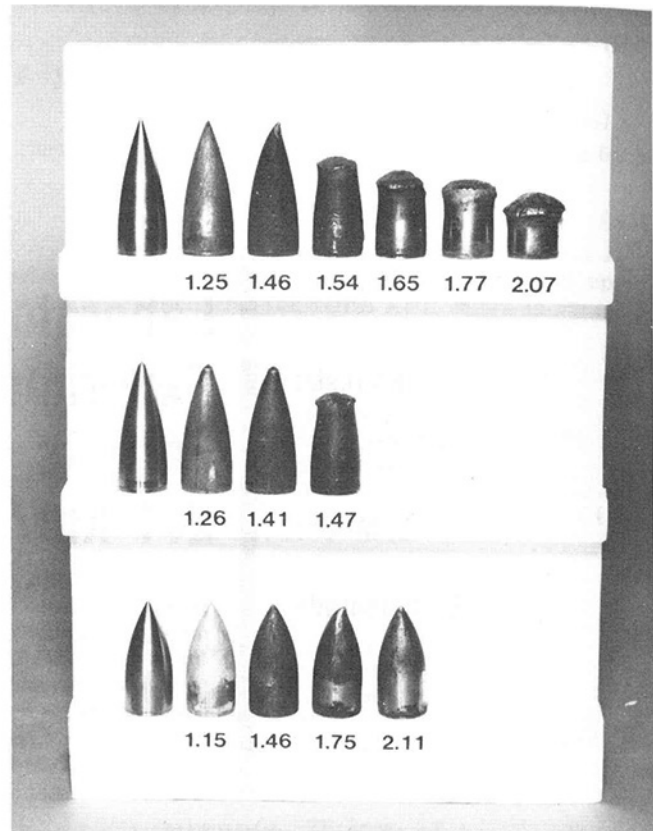
the mixture is oven fired, the material resembles a low-density cemented sandstone with nominal density 1.85 Mg/m^3 and porosity 30 percent. Triaxial material tests data for this material are published (Forrestal et al., 1984). As typical for dry geologic materials, shear resistance increases significantly with increasing confining pressure.

As shown in Fig. 2, polyurethane holders, designed to ensure normal impact and offer negligible axial constraint, supported the penetrators. Thin (0.25 mm, 0.01 in.) steel tubes held the nose shapes forward of the polyurethane holders to permit full-length·penetration of the foundry core targets before the projectile struck the back of the holders. These tubes were 246 mm (6.25 in.) long and were about nine percent of the total penetrator masses.

For the powder-gun experiments (impact velocity greater than 1.2 km/s), 69 mm diameter (2.7 in.), 121 mm length (4.75 in.) foundry core samples were contained in linen-phenolic projectiles with aluminum base plates. The gas-gun experiments used aluminum projectiles and 89 mm diameter, 89 mm length foundry core samples. At both facilities, impact velocities were measured to within 0.2 percent accuracy with a series of electrical contact pins.

Penetrators. The nose shapes shown in Fig. 1 were made from a dense (18.7 Mg/m^3) tungsten alloy.[1] These shapes consisted of a 6.0 CRH, a tip-modified 6.0 CRH, or a 3.0 CRH section and a stepped-cylindrical section. As illustrated in Fig. 2, the thin (0.25 mm) supporting tubes were shrunk fit to the nose shapes. All penetrators had 20.6 mm diameter afterbodies and masses of about 0.22 kg. Figure 2 illustrates the set-up for experiments that used laser interferometry to measure nose responses. As previously mentioned, some experiments were also conducted with piezoelectric ac-

---

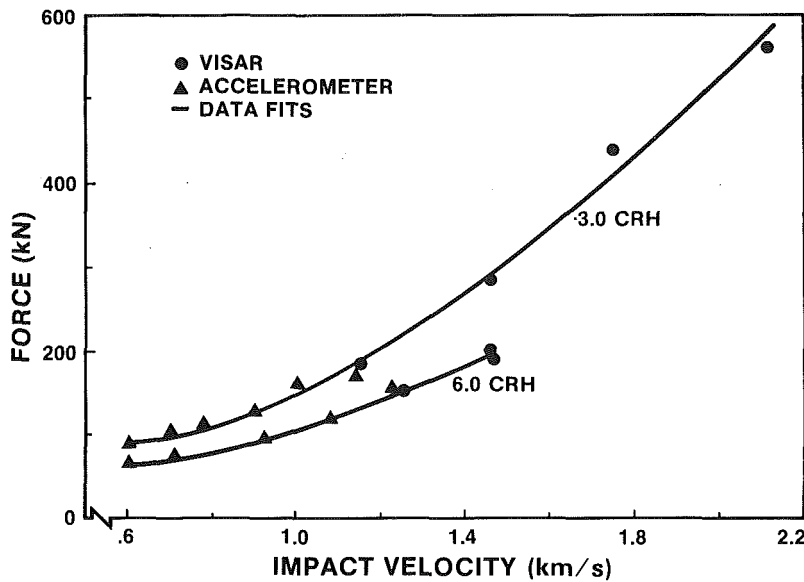[1]Kennertium W-2, Kennametal Inc., Latrobe, Pa. 15650.
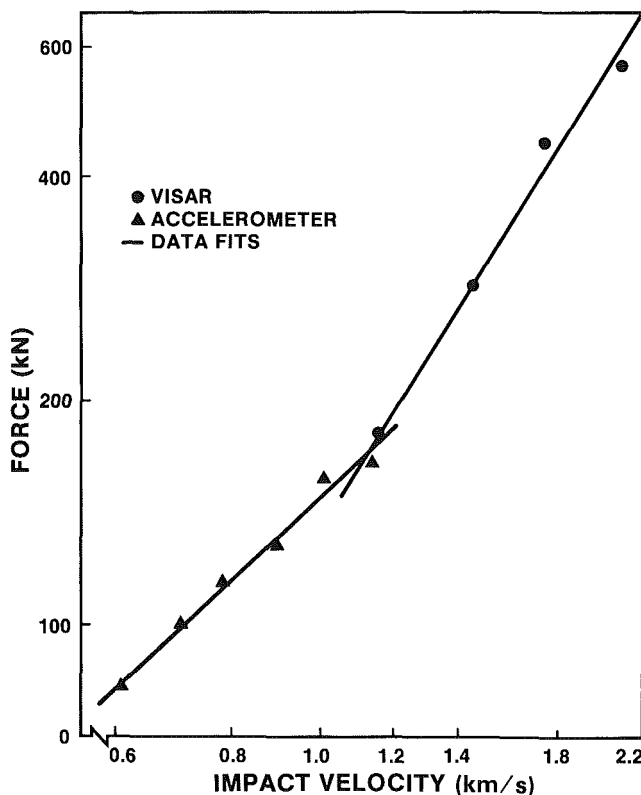
Fig. 5 Peak force versus impact velocity

Fig. 6 Measurements and data fits for the 3.0 CRH nose shape

Table 1 Data summary for the 3.0 CRH ogival-nosed penetrators with cylindrical diameter 20.6 mm (0.810 in.); (GG = gas gun, PG = powder gun, A = accelerometer, V = VISAR)

Impact Velocity (km/s)	Target Density (Mg/m³)	Facility, Measurement	Penetrator Mass (kg)	Peak Acceleration (g)	Peak Force (kN)
0.608	1.83	GG, A	228	37,000	82
0.704	1.83	GG, A	229	44,000	99
0.785	1.86	GG, A	229	50,000	113
0.895	1.85	GG, A	229	57,000	128
1.01	1.86	GG, A	228	70,000	158
1.14	1.84	GG, A	228	73,000	165
1.15	1.77	GG, V	217	85,000	181
1.46	1.85	PG, V	210	138,000	283
1.75	1.86	PG, V	220	203,000	440
2.11	1.84	PG, V	223	256,000	560

Table 2 Data summary for the 6.0 CRH ogival-nosed penetrators with cylindrical diameter 20.6 mm (0.810 in.); (GG = gas gun, PG = powder gun, V = VISAR, O = ogival tip, C = conical tip)

Impact Velocity (km/s)	Target Density (Mg/m³)	Facility, Measurement, Nose Tip	Penetrator Mass (kg)	Peak Acceleration (g)	Peak Force (kN)
1.10	1.84	GG, V, O	214	60,000	127
1.25	1.85	PG, V, O	218	72,000	153
1.26	1.80	PG, V, C	219	73,000	156
1.41	1.81	PG, V, C	218	83,000	178
1.46	1.85	PG, V, O	223	87,000	190
1.46	1.84	PG, V, O	220	92,000	198

wave studies. Therefore, for these relatively low-velocity measurements, we used an air-delay-leg VISAR (Amery, 1976, and Kusher et al., 1981) that was about five times more sensitive than VISARs used for shock wave studies and provided 3–5 fringes. Briefly, the interferometer provided a fringe signal with a fringe count proportional to the back surface velocity of the nosepiece. For the Argon–Ion laser and the delay length used for these experiments, each fringe corresponded to 0.031 km/s velocity change. Typical velocity-time data are presented in Fig. 3. Details on the acceleration measurement are contained in our previous paper (Forrestal et al., 1984).

Experimental Results

Figures 4–6 and Tables 1 and 2 summarize the results of this study. The post-test photographs[3] shown in Fig. 4 indicate clearly that the 6.0 CRH and tip-modified 6.0 CRH nose shapes exhibit severe, permanent deformations for impact velocities larger than 1.5 km/s. Brooks (1974) observed this same effect when he conducted experiments with 6.0 CRH, tungsten-alloy penetrators and AISI 4340 steel targets. That is,

celerometers.[2] For these experiments the accelerometers were screwed into the back of the nose shapes (Forrestal et al., 1984).

Measurements. Rigid-body velocity and acceleration were measured with laser interferometry (VISAR) and accelerometers, respectively. Laser interferometry (VISAR, Barker and Hollenbach, 1972) was developed to measure time-resolved motion of the back surface of shocked specimen. VISAR is a widely used precision tool for shock profile measurements. However, our experiments were concerned with rigid-body motions and the back surface velocity magnitudes were much lower than those for typical shock

---

[2]PCB Model 305A, PCB Piezotronics Inc., Depew, N.Y. 14043.

[3]We were not able to provide a soft catch for the penetrators. After impact, the penetrators interacted with a series of baffel plates.

in excess of a particular impact velocity the nose shape changed from essentially nondeforming to one that exhibited plastic flow. Brooks (1974) called this impact velocity, the hydrodynamic transition velocity. By contrast, the 3.0 CRH nose shape remained undeformed for impact velocities to 2.1 km/s.

We first conducted experiments with the 3.0 and 6.0 CRH shapes shown in Figs. 1a and 1c. The tip-modified, 6.0 CRH shape shown in Fig. 1b was designed with the intent of increasing the hydrodynamic transition velocity. However, subsequent experiments showed that this tip modification had no measurable effect. Figure 1d compares profiles of the 3.0 CRH and tip-modified 6.0 CRH nose shapes. The close similarity of these shapes indicates that the hydrodynamic transition velocity is sensitive to small geometry changes in nose shape.

Velocity-time profiles shown in Fig. 3 for the 6.0 CRH nose shapes provide additional information about the hydrodynamic transition velocity. The 1.25 km/s impact velocity was below the transition velocity, and velocity time was nearly linear after nose entry and before the end of travel through the foundry core target. However, the 1.77 km/s impact velocity was above the hydrodynamic transition velocity, and the velocity-time profile exhibited a monotonic slope increase after 40 μs. This velocity-time profile suggests that the onset time for the transition from a nondeformable nose to a plastically deformed nose shape was 40 μs.

As previously discussed, rigid-body velocity and acceleration of the nose shapes were measured with laser interferometry (VISAR) and accelerometers, respectively. Most of the experiments were conducted at impacts below the hydrodynamic transition velocity. For these experiments, velocity response was a smooth rise for about the time of nose entry followed by a nearly constant slope. This slope was measured to obtain peak acceleration and used to calculate peak force. Details of the acceleration measurements are discussed in our previous paper (Forrestal et al., 1984). Briefly, the rigid-body acceleration data show a smooth monotonic rise for about the time of nose entry followed by a nearly flat plateau. The magnitudes of the measured plateaus were used to calculate peak force. Tables 1 and 2 summarize the penetration data below the hydrodynamic transition velocity. Penetrator masses included the masses of the nose shape, supporting shell (0.02 kg), and accelerometer (0.005 kg, when applicable).

Peak force versus impact velocity data and quadratic fits to the data are shown in Fig. 5 for both the 3.0 and 6.0 CRH[4] nose shapes. The curve for the 6.0 CRH shape stops at $V = 1.5$ km/s, the hydrodynamic transition velocity. Data for the tip-modified, 6.0 CRH nose shape (Fig. 1b) are presented in Table 1, and these data show no measurable differences between the tip-modified 6.0 CRH and the 6.0 CRH nose shapes. It should also be pointed out that at $V = 1.5$ km/s (the

transition velocity for the 6.0 CRH nose shape), the force on the 3.0 CRH nose shape was 50 percent larger than that on the 6.0 CRH nose shape. We have, at this time, no explanation for this observation.

Data and linear fits to the data for the 3.0 CRH nose shape are also presented on a log-log plot in Fig. 6. Empirical models are widely used as predictive tools (Sliter, 1980), and these data can be described conveniently in the form

$$F = KV^n$$

and $K = 148$ and $n = 1.18$ for $0.61 < V < 1.14$, $K = 134$ and $n = 1.98$ for $1.14 < V < 2.11$, and F, V have the units of kN, km/s.

Discussion

Over the last two decades, hundreds of instrumented, full-scale, field tests into geological targets have been conducted. To complement these full-scale test programs, we have devised some laboratory-scale experiments that measure penetrator motion for impact velocities to 2.1 km/s. Since data for instrumented, field tests are currently limited to impact velocities of about 0.6 km/s, only laboratory-scale experiments can currently provide time-resolved, velocity, and acceleration data for higher impact velocities.

Acknowledgment

References

Amery, B. T., 1976, "Wide Range Velocity Interferometer," *Proceedings of the Sixth Symposium on Detonation*, Office of Naval Research Report No. ACR 221, Washington, D.C., pp. 681–689.

Backman, M. E., and Goldsmith, W., 1978, "The Mechanics of Penetration of Projectiles into Targets," *International Journal of Engineering Science*, Vol. 16, pp. 1–99.

Barker, L. M., and Hollenbach, R. E., 1972, "Laser Interferometer for Measuring High Velocities of Any Reflecting Surface," *Journal of Applied Physics*, Vol. 43, No. 11, pp. 4669–4675.

Brooks, P. N., 1974, "Ballistic Impact—The Dependence of the Hydrodynamic Transition Velocity on Projectile Tip Geometry," DREV Report 4001/74, Research and Development Branch, Dept. of National Defense, Quebec, Canada.

Forrestal, M. J., Longcope, D. B., and Norwood, F. R., 1981, "A Model to Estimate Forces on Conical Penetrators Into Dry Porous Rock," ASME JOURNAL OF APPLIED MECHANICS, Vol. 48, pp. 25–29.

Forrestal, M. J., Lee, L. M., Jenrette, B. D., and Setchell, R. E., 1984, "Gas-Gun Experiments Determine Forces on Penetrators Into Geological Targets," ASME JOURNAL OF APPLIED MECHANICS, Vol. 51, No. 3, pp. 602–607.

Kusher, G., Hohler, V., Stilp, A., and Schneider, E., 1981, "Laser-Interferomic Investigations of Rod Deceleration During Impact Process," *Proceedings of the Sixth International Symposium on Ballistics*, Orlando, Florida.

Longcope, D. B., and Forrestal, M. J., 1983, "Penetration of Targets Described by a Mohr–Coulomb Failure Criterion With a Tension Cutoff," ASME JOURNAL OF APPLIED MECHANICS, Vol. 50, No. 2, pp. 327–333.

Sliter, G. E., 1980, "Assessment of Empirical Concrete Impact Formulas," *Journal of the Structural Division*, ASCE, ST5, pp. 1023–1045.

Young, C. W., 1969, "Depth Prediction For Earth Penetrating Projectiles," *ASCE Journal of Soil Mechanics and Foundation*, Vol. 95, No. SM3, pp. 803–817.

Young, C. W., and Keck, L. J., 1971, "An Air-Dropped Sea Ice Penetrometer," SC-DR-71-0729, Sandia National Laboratories, Albuquerque, N.M.

Zukas, J. A., et al., 1982, *Impact Dynamics*, Wiley, New York.

---

[4]Accelerometer data for the 6.0 CRH nose shape were taken from our previous paper (Forrestal et al., 1984).